Supporting Information

Combined electrochemical and DFT investigations of iron selenide: a mechanically bendable solid-state symmetric supercapacitor

Bidhan Pandit[1,2], Sachin R. Rondiya[3], Shyamal Shegokar[1], Lakshmana K. Bommineedi[1], Russel W. Cross[3], Nelson Y. Dzade[3], Babasaheb R. Sankapal[1]*

[1]Nano Materials and Device Laboratory, Department of Physics, Visvesvaraya National Institute of Technology, South Ambazari Road, Nagpur 440010, Maharashtra, India.

[2]Department of Materials Science and Engineering and Chemical Engineering, Universidad Carlos III de Madrid, Avenida de la Universidad 30, 28911 Leganés, Madrid, Spain.

[3]School of Chemistry, Cardiff University, Main Building, Park Place, Cardiff, CF10 3AT, Wales, United Kingdom.

Corresponding author footnote

Babasaheb R. Sankapal

E-mail: brsankapal@phy.vnit.ac.in; brsankapal@gmail.com

Tel.: +91 (712) 2801170; Fax No.: +91 (712) 2223230

Supporting Discussion

Specific capacitance from the CV curves was calculated with the help of following formula[1]:

$$C_s = \frac{1}{2mv\Delta V}\int_{V_i}^{V_f} I(V)dV \qquad (1)$$

where, 'C_s' signifies the specific capacitance (F/g), 'm' indicates mass (g) deposited on SS substrate, 'v' specifies scan rate (V), 'ΔV' is the functional potential frame and '$\int_{V_i}^{V_f} I(V)dV$', represents area under the CV curve.

Specific capacitance (C_s), specific energy (E) in Wh/kg and specific power (P) in W/kg from Galvanostatic charge-discharge can be calculated using following equations [2]:

$$C_s = \frac{I\Delta t}{m\Delta V} \qquad (2)$$

$$E = \frac{1}{2}\left[\frac{C_s \Delta V^2}{3.6}\right] \qquad (3)$$

$$P = \frac{3600 \times E}{\Delta t} \qquad (4)$$

where, 'I' represents current intensity and 'Δt' denotes discharge time (t) of the experimental charge-discharge curve.

For a two-electrode supercapacitor device, two electrodes are sandwiched with a separator in between them. In our case, the gel electrolyte works both as electrolyte and separator. So, the full cell is considered as the series combination of two capacitors. Hence,

the total capacitance (C_{cell}) is calculated according to Equation (5), in which C_+ and C_- are the capacitances of the associated two electrodes, respectively:

$$\frac{1}{C_{cell}} = \frac{1}{C_+} + \frac{1}{C_-} \quad (5)$$

For a symmetric system, $C_+ = C_- = C_{electrode}$

So, $$C_{cell} = \frac{C_{electrode}}{2} \quad (6)$$

Cell specific capacitance: $$C_{SP,\,cell} = \frac{C_{cell}}{m_{total}} = \frac{C_{electrode}}{2} * \frac{1}{2 * m_{electrode}} = \frac{C_{SP,\,electrode}}{4} \quad (7)$$

Where m_{total} is the total mass ($m_+ + m_-$) involved in cell.

As the cell configuration is symmetric, $m_+ = m_- = m_{electrode}$.

So, $m_+ + m_- = 2 * m_{electrode}$.

And again, $C_{SP,electrode} = C_{electrode}/m_{electrode}$.

So, it is obvious that the total specific capacitance of cell (2-electrode) will always one-fourth of the associated 3-electrode system.[3]

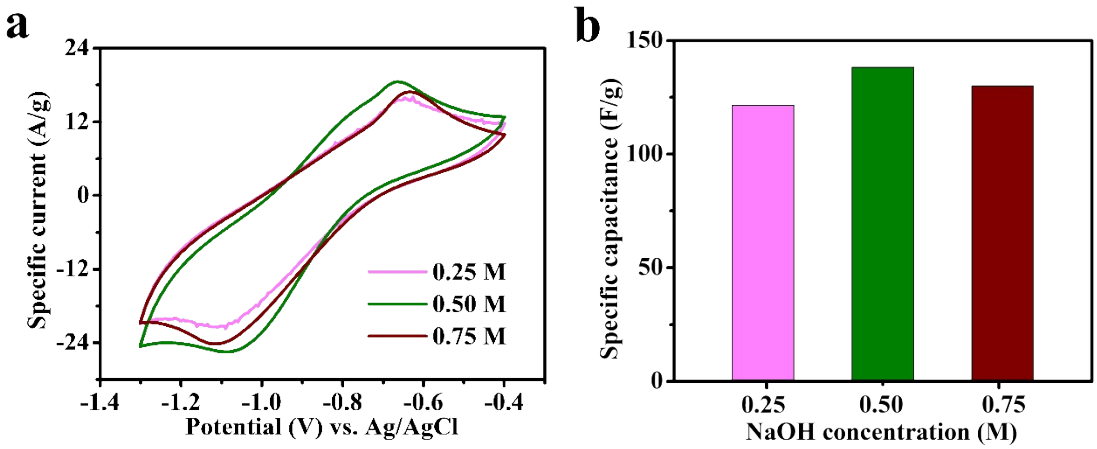

Figure S1 (a) CV curves for various NaOH concentrations. (b) Specific capacitance with associated NaOH concentrations.

The aqueous electrolyte concentration (NaOH) was changed to get optimized electrochemical behavior at scan rate of 100 mV/s with the potential window between -0.4 to -1.3 V (**Figure S1a**). The electrode shows maximum specific capacitance at 0.5 M NaOH aqueous electrolyte as shown in **Figure S1b**. Low concentration (0.25 M) can't provide sufficient electrolyte ions for electrochemical activities, whereas higher concentration (0.75 M) causes lower ionic mobility due to less water hydration, demonstrating capacitance drop in both the cases.[4]

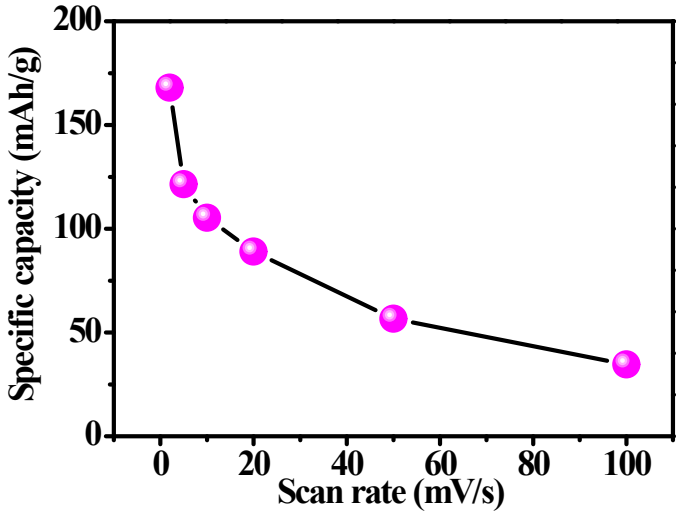

Figure S2 Specific capacity vs. scan rate plot of $FeSe_2$ electrode.

Moreover, the battery redox characteristics are totally different and more complex than pseudocapacitors. Here we are adding the mechanism of $FeSe_2$ electrode for Na-ion battery to distinguish from pseudocapacitor point of view. At scan rate of 2 mV/s, the same $FeSe_2$ electrode exhibits 167.9 mAh/g (**Figure S2**) which is very low from the theoretical capacity as anode point of view. In comparison to pseudocapacitive mechanism, the charge-discharge mechanism here is associated with conversion reactions.[5] In initial discharge, $FeSe_2$ reacts with Na^+ to form Se (elemental) and $Na_xFe_3Se_4$. In the following conversion reaction, $Na_xFe_3Se_4$ reacts with Na^+ to generate Na_2Se and Fe. During the charge step, initially formed Fe is transformed o the final product of Fe_3Se_4. In the next cycle, the conversion reaction among Fe_3Se_4 and Na_2Se occurs. So, the starring material $FeSe_2$ will never be get back after the 1st cycle.[6]

During discharge:

$$3FeSe_2 + xNa^+ + xe^- \rightarrow Na_xFe_3Se_4 + 2Se \qquad (8)$$

$$Na_xFe_3Se_4 + (8-x)Na^+ + (8-x)e^- \rightarrow 4Na_2Se + 3Fe \qquad (9)$$

During charge:

$$4Na_2Se + 3Fe \rightarrow Na_xFe_3Se_4 + (8-x)Na^+ + (8-x)e^- \qquad (10)$$

$$Na_xFe_3Se_4 \rightarrow Fe_3Se_4 + xNa^+ + xe^- \qquad (11)$$

Even this electrochemical reaction mechanism is confirmed by the *in situ* XRD studies by Ge et al.[5]

Table S1: Gel electrolyte based symmetric solid-state supercapacitor devices

Electrode materials	Electrolyte	Voltage window (V)	Specific capacitance (F/g)	Maximum Specific energy (Wh/kg)	Maximum Specific power (kW/kg)	Cyclic stability		Ref.
						Retention (%)	Cycles	
Porous carbon	PVA-KOH	0.8	81.3	7.22	0.1	~90.2	6000	[7]
rGO-PEDOT/PSS	PVA-H_3PO_4	1	448 mF/cm^2	2.83	3.5895	95	10000	[8]
GO/PPy	LiCl-PVA	0.8	347.8 mF/cm^2	15.1	4	86	2000	[9]
MoS_2/carbon cloth	LiCl-PVA	1.6	368	5.42	0.128	96.5	5000	[10]
ZnS/CNTs	PVA-KOH	1	159.6	22.3	5	91.8	3000	[11]
SWCNTs/RuO_2	H_3PO_4-PVA	1	138	18.8	96	-	-	[12]
PEDOT:PSS/ MWCNT	PVA-KOH	1	380	13.2	4.99	90	1000	[13]
MWCNTs	PVA-H_3PO_4	1	26.8 F/g	3.5	28.1	92	5000	[14]
Waste paper fibers-RGO–MnO_2	PVA-Na_2SO_4	0.8	220	19.6	2.4	85.3	2000	[15]
$ZnCo_2O_4$/rGO	PVA-KOH	0.4	143	11.44	1.382	93.4	5000	[16]
NiS	PVA-$LiClO_4$	1.2	55.83	9.3	0.67	90	1500	[17]
V_2O_5	PVA-$LiClO_4$	1.8	358	43	3.604	88	1000	[18]
V_2O_5/ MWCNTs	PVA-$LiClO_4$	1.8	629	72.07	8.4	96	4000	[19]
CuS	PVA-$LiClO_4$	1.6	172.5	12	1.75	93	2000	[20]
VS_2/ MWCNTs	PVA-$LiClO_4$	1.6	182	42	4.8	93.2	5000	[21]
MnO_2	PVA-$LiClO_4$	1.6	110	23	7.692	92	2200	[22]
MnO_2	PVA-LiCl	0.8	776	-	-	91	20000	[23]
MWCNTs/ MnO_2	PVA-Na_2SO_4	1	204	28.33	-	80.36	2500	[24]
Graphene/ polyaniline	PVA-H_2SO_4	0.8	665	-	-	100	10000	[7]
SWCNTs/ TiO_2	PVA-LiCl	0.8	28	-	66.7	100	1000	[25]
$FeSe_2$	**PVA-$LiClO_4$**	**1.8**	**65.3**	**13.4**	**5.1**	**-**	**-**	**Present work**

References

1. C. Niu, G. Han, H. Song, S. Yuan and W. Hou, *J. Colloid Interface Sci.*, 2020, **561**, 117-126.
2. S. Maitra, R. Mitra and T. K. Nath, *Curr. Appl. Phys.*, 2020, **20**, 628-637.
3. S. Roldan, D. Barreda, M. Granda, R. Menendez, R. Santamaria and C. Blanco, *Phys. Chem. Chem. Phys.*, 2015, **17**, 1084-1092.
4. K.-C. Tsay, L. Zhang and J. Zhang, *Electrochim. Acta*, 2012, **60**, 428-436.
5. J. Ge, B. Wang, J. Wang, Q. Zhang and B. Lu, *Adv. Energy Mater.*, 2020, **10**, 1903277.
6. Q. Yu, B. Jiang, J. Hu, C.-Y. Lao, Y. Gao, P. Li, Z. Liu, G. Suo, D. He, W. Wang and G. Yin, *Adv. Sci.*, 2018, **5**, 1800782.
7. X. Li, K. Liu, Z. Liu, Z. Wang, B. Li and D. Zhang, *Electrochim. Acta*, 2017, **240**, 43-52.
8. Y. Liu, B. Weng, J. M. Razal, Q. Xu, C. Zhao, Y. Hou, S. Seyedin, R. Jalili, G. G. Wallace and J. Chen, *Sci. Rep.*, 2015, **5**, 17045.
9. J. Cao, Y. Wang, J. Chen, X. Li, F. C. Walsh, J.-H. Ouyang, D. Jia and Y. Zhou, *J. Mater. Chem. A*, 2015, **3**, 14445-14457.
10. M. S. Javed, S. Dai, M. Wang, D. Guo, L. Chen, X. Wang, C. Hu and Y. Xi, *J. Power Sources*, 2015, **285**, 63-69.
11. X. Hou, T. Peng, J. Cheng, Q. Yu, R. Luo, Y. Lu, X. Liu, J.-K. Kim, J. He and Y. Luo, *Nano Res.*, 2017, **10**, 2570-2583.
12. P. Chen, H. Chen, J. Qiu and C. Zhou, *Nano Res.*, 2010, **3**, 594-603.
13. D. Zhao, Q. Zhang, W. Chen, X. Yi, S. Liu, Q. Wang, Y. Liu, J. Li, X. Li and H. Yu, *ACS Appl. Mater. Interfaces*, 2017, **9**, 13213-13222.

14. S. Li, C. Xuebo, L. Lei, W. Qiaodi, Y. Huating, G. Li, M. Changjie, S. Jiming, Z. Shengyi and N. Helin, *Adv. Funct. Mater.*, 2017, **27**, 1700474.

15. H. Su, P. Zhu, L. Zhang, F. Zhou, G. Li, T. Li, Q. Wang, R. Sun and C. Wong, *J. Electroanal. Chem.*, 2017, **786**, 28-34.

16. M. I. Kyu, Y. Seonno and O. Jungwoo, *Chem. Eur. J.*, 2017, **23**, 597-604.

17. A. M. Patil, A. C. Lokhande, N. R. Chodankar, V. S. Kumbhar and C. D. Lokhande, *Mater. Des.*, 2016, **97**, 407-416.

18. B. Pandit, D. P. Dubal and B. R. Sankapal, *Electrochim. Acta*, 2017, **242**, 382-389.

19. B. Pandit, D. P. Dubal, P. Gómez-Romero, B. B. Kale and B. R. Sankapal, *Sci. Rep.*, 2017, **7**, 43430.

20. A. M. Patil, A. C. Lokhande, N. R. Chodankar, P. A. Shinde, J. H. Kim and C. D. Lokhande, *J. Ind. Eng. Chem.*, 2017, **46**, 91-102.

21. B. Pandit, S. S. Karade and B. R. Sankapal, *ACS Appl. Mater. Interfaces*, 2017, **9**, 44880-44891.

22. N. R. Chodankar, D. P. Dubal, G. S. Gund and C. D. Lokhande, *Journal of Energy Chemistry*, 2016, **25**, 463-471.

23. R. Soni, A. Raveendran and S. Kurungot, *Nanoscale*, 2017, **9**, 3593-3600.

24. N. R. Chodankar, S.-H. Ji and D.-H. Kim, *J. Taiwan Inst. Chem. Engrs.*, 2017, **80**, 503-510.

25. C. Chen, C. Jun, L. Qiongqiong, W. Xinyu, S. Li, N. Zhiqiang and C. Jun, *Adv. Funct. Mater.*, 2017, **27**, 1604639.